Mapping Out Atom-Wall Interaction with Atomic Clocks

A. Derevianko,[1] B. Obreshkov,[1] and V. A. Dzuba[1,2]

[1]*Department of Physics, University of Nevada, Reno, Nevada 89557, USA*
[2]*School of Physics, University of New South Wales, Sydney, 2052, Australia*

(Received 27 May 2009; published 23 September 2009)

We explore the feasibility of probing atom-wall interaction with atomic clocks based on atoms trapped in engineered optical lattices. Optical lattice is normal to the wall. By monitoring the wall-induced clock shift at individual wells of the lattice, one would measure the dependence of the atom-wall interaction on the atom-wall separation. We find that the induced clock shifts are large and observable at already experimentally demonstrated levels of accuracy. We show that this scheme may uniquely probe the long-range atom-wall interaction in all three qualitatively distinct regimes of the interaction: van der Waals (image-charge interaction), Casimir-Polder (QED vacuum fluctuations), and Lifshitz (thermal-bath fluctuations) regimes.

DOI: 10.1103/PhysRevLett.103.133201 PACS numbers: 34.35.+a, 06.30.Ft, 37.10.Jk

Atomic clocks define the unit of time, the second. Usually environmental effects (e.g., stray fields) degrade the performance of the clocks. One may turn this around and by measuring shifts of the clock frequency, characterize an interaction with the environment. The most fundamental experiments of this kind search for a potential variation of fundamental constants [1], where the ''environmental agent'' is the fabric of the Universe itself, affecting the rate of ticking of atomic clocks. In this Letter, we evaluate a feasibility of using atomic clocks to measure basic laws of atom-wall interactions. We find that a certain class of atomic clocks, the optical lattice clocks, are capable of accurately characterizing the atom-wall interaction. Moreover, this is a unique system where the atom-wall interaction may be probed in all three qualitatively distinct regimes of the interaction in a single experiment: van der Waals (image-charge interaction), Casimir-Polder (QED vacuum fluctuations), and Lifshitz (thermal-bath fluctuations).

Understanding the basic atom-wall interaction [2] is important, for example, for probing a hypothetical ''non-Newtonian'' gravity at a μm scale (see, e.g., Ref. [3]). Also, with miniaturization of atomic clocks, for example, using atomic chips [4], the atom-wall interaction may become an important systematic issue.

In optical lattice clocks, ultracold atoms are trapped in minima (or maxima) of intensity of a standing wave of a laser light operated at a certain ''magic'' wavelength [5,6]. The lattice wavelength is tuned so that the differential light perturbations of the two clock levels vanishes exactly. Such ideas were experimentally realized [7–9] for divalent atoms, such as Sr, yielding fractional accuracies at a 10^{-16} level [9]. The clock transition is between the ground $^1S_0$ and the lowest-energy excited $^3P_0$ state.

An idealized setup for measuring atom-wall interaction is shown in Fig. 1. A conducting surface of interest acts as a mirror for the laser beam normally incident on the surface. The resulting interference of the beams forms an optical lattice. Laser operates at a magic wavelength λ_m specific to the atom (see Table I). For all tabulated λ_m, atoms are attracted to maxima of the laser intensity and one could work with 1D optical lattices. The first pancake-shaped atomic cloud would form at $\lambda_m/4$ distance from the mirror. The subsequent adjacent clouds are separated by a distance $\lambda_m/2$. Reference [12] discusses an experimental procedure for loading atoms into sites close to a mirror.

Two earlier proposals, by Florence [12] and Paris [13] groups, considered trapping divalent atoms in optical lattices for studying atom-wall interaction. In both proposals

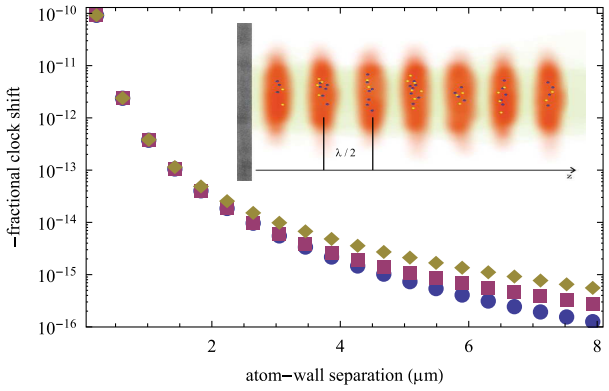

FIG. 1 (color online). Inset: Idealized setup for measuring atom-wall interaction with optical lattice clocks. Clouds of ultracold atoms are trapped in an optical lattice operating at a ''magic'' wavelength. By monitoring the wall-induced clock shift at individual trapping sites, one measures a dependence of the atom-wall interaction on the atom-wall separation. Main figure: Fractional clock shifts for Sr as a function of separation from a gold surface at three temperatures, $T = 77$ K (blue dots), $T = 300$ K (red squares), and $T = 600$ K (brown diamonds). Individual points represent shifts in individual trapping sites of the optical lattice. The first well is placed at $\lambda_m/4$ and subsequent points are separated by $\lambda_m/2$.

TABLE I. Fractional shifts of the $^1S_0 - {}^3P_0$ clock transitions in divalent atoms due to the presence of an ideal conducting surface. The second column lists clock frequencies. Values of magic wavelengths, λ_m, in Sr and Yb are experimental [10,11] and are our theoretical results for other atoms. The differences of the static polarizabilities $\alpha(0)$ and the van der Waals coefficients C_3 for the two clock levels are tabulated in the fourth and fifth columns. Finally, we list the fractional-shift parameters $\beta_{\rm CP}$, $\beta_{\rm vdW}$, and β_L, Eq. (5). Notation $a[b]$ stands for $a \times 10^b$.

Atom	$\nu_{\rm clock}$, Hz	λ_m, nm	$\Delta\alpha(0)$, a.u.	ΔC_3, a.u.	$\beta_{\rm vdW}$	$\beta_{\rm CP}$	β_L
Mg	6.55[14]	466	29	0.21	−3.1[−12]	−7.9[−13]	−1.0[−13]
Ca	4.54[14]	739	138	0.17	−8.8[−13]	−8.6[−13]	−1.8[−13]
Sr	4.29[14]	813	261	0.25	−1.1[−12]	−1.2[−12]	−2.6[−13]
Yb	5.18[14]	759	155	0.35	−1.5[−12]	−7.6[−13]	−1.6[−13]
Zn	9.69[14]	416	28	0.30	−4.2[−12]	−8.2[−13]	−9.4[−14]
Cd	9.03[14]	419	28	0.31	−4.6[−12]	−8.7[−13]	−1.0[−13]
Hg	1.13[15]	362	22	0.30	−5.5[−12]	−9.8[−13]	−9.8[−14]

the lattices are oriented vertically and ultracold atoms experience a combination of periodic optical potential and linear gravitational potential. In the Florence proposal [12], the atom-wall interaction modifies Bloch oscillation frequencies of atomic wave packets in this potential. In the Paris proposal [13], laser pulses at different frequencies are used to create an interferometer with a coherent superposition of atomic wave packets at different sites; the experiment is sensitive to a difference of atom-wall interaction at spatially separated sites. Here we explore an alternative: we consider using *atomic clocks* operating in magic lattices. By monitoring the clock shift at individual trapping sites, one measures a distance dependence of the atom-wall interaction.

Qualitative estimates.—As the separation z between an atom and a wall increases, the atom-wall interaction evolves through several distinct regimes: (i) chemical-bond region that extends a few nm from the surface, (ii) van der Waals (vdW) region, (iii) retardation [Casimir-Polder (CP)] region, and (iv) the thermal (Lifshitz) zone. The chemical-bond region is beyond the scope of our Letter and we focus on the three longer-range regimes of the interaction between a perfectly conducting wall and a spherically symmetric atom.

Qualitatively, the vdW interaction arises due to an interaction of atomic electrons and nucleus with their image charges

$$U_{\rm vdW}(z) = -C_3 z^{-3}, \tag{1}$$

where the coefficient C_3 depends on an atomic state. It may be expressed in terms of the electric-dipole dynamic polarizability of the atom as

$$C_3 = \frac{1}{4\pi}\int_0^\infty \alpha(i\omega)d\omega. \tag{2}$$

Equation (1) assumes instantaneous exchange of virtual photons. More rigorous QED consideration leads to the Casimir-Polder limit [14]

$$U_{\rm CP}(z) = -3/(8\pi)\hbar c\alpha(0)z^{-4}. \tag{3}$$

A transition between the vdW and the CP regions occurs at the length scale $\hbar c/\Delta E_a$, where ΔE_a is a characteristic value of the atomic resonance excitation energy.

The CP interaction, Eq. (3), is mediated by vacuum fluctuations of electromagnetic field. At finite temperatures T, populations of the vacuum modes are modified and a new length scale, $\hbar c/(k_B T)$, appears. As shown by Lifshitz [15], the interaction becomes

$$U_L(z) = -1/4k_b T\alpha(0)z^{-3}. \tag{4}$$

Because of the interaction with the wall, both clock levels would shift. We may parametrize the resulting fractional clock shifts as

$$\frac{\delta\nu}{\nu_{\rm clock}}(z,T) = \begin{cases} \beta_{\rm vdW}(\frac{\lambda_m}{z})^3, \\ \beta_{\rm CP}(\frac{\lambda_m}{z})^4, \\ \beta_L(\frac{T}{300\ {\rm K}})(\frac{\lambda_m}{z})^3. \end{cases} \tag{5}$$

We evaluated coefficients β for the clock transitions in Mg, Ca, Sr, Yb, Zn, Cd, and Hg (see discussion of the method later on). The results are presented in Table I. The estimates of Table I immediately show that the atom-wall interaction is a large effect, corresponding to 10^{-10} fractional clock shifts at the first well. This is roughly 10^6 times larger than the demonstrated accuracy of the Sr clock [9].

Rigorous consideration.—In general, as the atom-wall separation is varied, there is a smooth transition between the three interaction regimes. To properly describe the crossover regions, we employ an expression by Babb *et al.* [16], which may be represented as

$$U(z,T) = -\frac{k_B T}{4z^3}\left[\alpha(0) + \sum_{l=1}^{\infty}\alpha(i\xi_l)I\left(\xi_l\frac{2z}{c}, \frac{c}{2z\omega_p}\right)\right], \tag{6}$$

where the atomic dynamic polarizability is convoluted with $I(\zeta,\chi) = (1+\zeta^2\chi^2)\Gamma(3,\zeta) + \zeta^4\chi\Gamma(0,\zeta) - 3\zeta^2\chi\Gamma(2,\zeta) + 2\zeta^4\chi^2\Gamma(1,\zeta) - \zeta^6\chi^2\Gamma(-1,\zeta)$ at Matsubara frequencies

$$\xi_l = (2\pi k_B T/\hbar)\times l, \qquad l = 0, 1, 2, \ldots,$$

$\Gamma(n, \zeta)$ being the incomplete gamma function. In addition to recovering various limiting cases, Eq. (6) also accounts for realistic properties of conducting wall (described by plasma frequency ω_p).

Atomic properties enter the atom-wall interaction through the dynamic electric-dipole polarizability of imaginary frequency $\alpha(i\omega)$. For the two clock levels the perturbation of the clock frequency may be expressed in terms of the difference $\Delta\alpha(i\omega) = \alpha_{^3P_0}(i\omega) - \alpha_{^1S_0}(i\omega)$. We computed the polarizabilities using the *ab initio* relativistic configuration interaction method coupled with many-body perturbation theory. The summation over intermediate states entering the polarizability was carried out using the Dalgarno-Lewis method. Details of the formalism may be found in Ref. [17]. Detailed dynamic polarizabilities $\alpha(i\omega)$ and C_3 coefficients for the ground states of alkaline-earth atoms may be found in Ref. [18]. A comprehensive analysis of the accuracy of calculations for Yb is presented in our forthcoming paper [19]; it is at the level of 10%. Among atoms compiled in Table I, Yb has the most electrons and thus the most complicated structure; we expect that the relative accuracy for other atoms does not exceed several per cent.

Dynamic polarizabilities of Sr atom are shown in Fig. 2. Notice that the individual polarizabilities $\alpha_{^3P_0}(i\omega)$ and $\alpha_{^1S_0}(i\omega)$ slowly decrease as ω increases. At large frequencies each polarizability approaches *the same* asymptotic limit $\alpha(i\omega) \sim N_e/\omega^2$, N_e being the number of atomic electrons. As a result, compared to the individual $\alpha(i\omega)$, the differential polarizability, $\Delta\alpha(i\omega)$, is strongly peaked around $\omega = 0$. Only the Matsubara frequencies inside this peak are relevant in Eq. (6). Curiously, $\Delta\alpha(i\omega)$ passes through zero at $\omega \approx 0.05$ a.u. This is reminiscent of the magic frequency for the perturbation of the clock transition by laser field which is expressed in terms of differential polarizability of *real* argument, $\Delta\alpha(\omega)$.

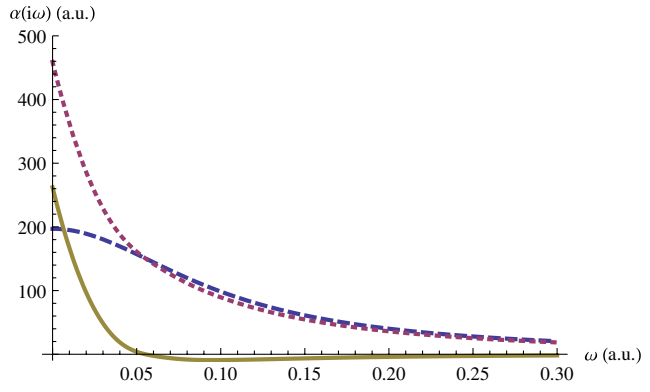

FIG. 2 (color online). Dynamic polarizabilities of imaginary frequency $\alpha(i\omega)$ of the Sr clock levels, $5s5p^3P_0$ (dotted line) and $5s^{21}S_0$ (dashed line) as a function of frequency. Differential polarizability $\Delta\alpha(i\omega) = \alpha_{^3P_0}(i\omega) - \alpha_{^1S_0}(i\omega)$ is shown with a solid line. All quantities are in atomic units.

With the computed $\Delta\alpha(i\omega)$, we evaluate the atom-wall clock shifts, Eq. (6). We use plasma frequency $\omega_p = 9$ eV (gold wall) and consider several temperatures $T = 77, 300$, and 600 K. Results for the Sr clock are shown in Fig. 1. Individual points represent shifts in individual wells of the optical lattice. Roughly the first 20 wells produce a fractional clock shift above the already demonstrated 10^{-16} accuracy limit [9]. We observe that over 20 wells the clock shift varies by 6 orders of magnitude. As the temperature of the surface is increased, the clock shifts become more pronounced.

It is worth pointing out that Eq. (6) assumes that the temperatures of the environment and the wall are the same (otherwise, see Refs. [20,21]). Moreover, the clock shifts in Fig. 1 do not include the conventional black-body-radiation shifts [22].

Lattice clocks are sensitive to long-range atom-wall interactions in all three regimes: van der Waals, retardation (Casimir-Polder), and thermal-bath (Lifshitz) regimes. Indeed, in Fig. 3 we draw a ratio

$$\eta(z, T) = U(z, T)/U_{\mathrm{CP}}(z). \tag{7}$$

Parameter η is equal to one in the region where the CP approximation is valid. From Fig. 3, we observe that the transition between the vdW and the CP regimes occurs around well number 4. The position of the second transition region, from the CP to the Lifshitz regimes, depends on the temperature. For $T = 77$ K, this crossover is delayed until well number 25 (not shown on the Fig. 3). $T = 600$ K represents another extreme, as the vdW region immediately transforms into the Lifshitz region. Atom-wall interaction at room temperature, $T = 300$ K, represents an intermediate case, where the CP approximation is valid over several wells, and all the three domains become distinguishable.

We showed that the lattice clocks can be used to detect all three qualitative-distinct mechanisms

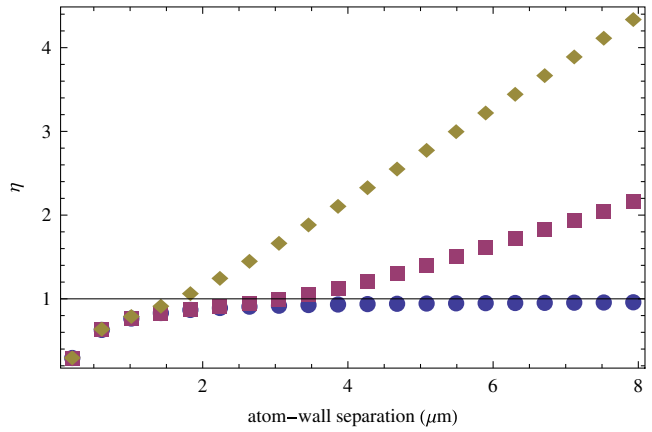

FIG. 3 (color online). Sr clock shift of Fig. 1 normalized to the Casimir-Polder limit, Eq. (7) at $T = 77$ K (blue dots), $T = 300$ K (red squares), and $T = 600$ K (brown diamonds).

of the atom-wall interaction. In this regard, the lattice clocks offer a unique opportunity to map out both van der Waals → Casimir-Polder and Casimir → Polder-Lifshitz transition regions. This distinguishes our clock proposal from previous experiments: the former transition was probed in Ref. [23], while the latter was detected in Ref. [21]. None of the experiments so far has been able to map out both transitions simultaneously.

Accuracy and atomic confinement.—Commonly, the accuracy of determination of the atom-wall interaction is limited by the spatial extent of an atomic ensemble [2]. An advantage of working with optical lattices lies with a tight spatial confinement at the lattice sites. Because of a variation of the atom-wall interaction over a trapping site, the clock shift acquires a width, leading to an uncertainty $\delta U(z,T)/U(z,T) \approx 0.3/N_w^2(E_r/V_0)^{1/2}$, where V_0 is the depth of the optical lattice and $E_r = \hbar^2(2\pi/\lambda_m)^2/(2M)$ is the photon recoil energy for an atom of mass M. N_w is the lattice site number counting from the surface. This uncertainty becomes smaller as N_w increases (potential becomes less steep) and as the ratio V_0/E_r increases (better confinement).

The ratio V_0/E_r can be increased by ramping up the intensity of the lattice laser. For a given accuracy of the clock, the limitation on the maximum of intensity arises from higher-order corrections to ac Stark effect (hyperpolarizability), experimentally studied in Ref. [24]. They found that V_0/E_r can be as high as 100 without affecting the performance of the clock at the 10^{-16} level. With this ratio, we find that for $N_w \approx 10$ the error in the determination of the atom-wall interaction due to imperfect confinement of the atoms can be as small as 0.1%.

For lattice sites near the wall, the accuracy can be improved by increasing V_0/E_r. As an example, consider the well number 2. The wall-induced clock shift here is $\sim 10^{-12}$ (see Fig. 1) and for a 1% measurement the clock may operate at the 10^{-14} accuracy level. At this level, the hyperpolarizability effect would require $V_0/E_r < 1000$ (the required laser intensity is feasible [24]), consistently translating into a sub-1% error in the determination of the atom-wall interaction.

The spread of the atomic wave function constrains performance of the earlier proposals for studying atom-wall interaction with optical lattices. For example, in the Bloch oscillation scheme of Ref. [12] the atomic cloud extends over many lattice sites; this limits that scheme to measurements at relatively large atom-wall separations. In Ref. [13] the performance of the interferometric measurements is optimized at $V_0/E_r \approx 5$, which is too small for accurately determining the interaction strength near the surface (requires $V_0/E_r \approx 1000$).

To conclude, here we explored a feasibility of using atomic clocks for measuring atom-wall interaction by monitoring wall-induced clock shift. We demonstrated that the exquisite accuracy of the clocks offers a unique opportunity to map out all three qualitatively distinct regimes of the long-range atom-wall interaction in a single experiment. None of the previous experiments was capable of measuring the interaction in all three regimes.

We thank J. Babb, J. Weinstein, H. Katori, G. Tino, P. Wolf, and A. Cronin for discussions and Issa Beckun for drawing the inset of Fig. 1. This work was supported in part by the NSF, NASA, and by the Australian RC.

[1] T. M. Fortier *et al.*, Phys. Rev. Lett. **98**, 070801 (2007).
[2] D. Bloch and M. Ducloy, in *Advances in Atomic, Molecular, and Optical Physics*, edited by B. Bederson and H. Walther (Academic, San Diego, 2005), Vol. 50, pp. 91–154.
[3] L. Randall, Science **296**, 1422 (2002).
[4] D. Gallego *et al.*, arxiv:0905.2207v1.
[5] H. Katori *et al.*, Phys. Rev. Lett. **91**, 173005 (2003).
[6] J. Ye, H. J. Kimble, and H. Katori, Science **320**, 1734 (2008).
[7] M. Takamoto *et al.*, Nature (London) **435**, 321 (2005).
[8] R. Le Targat *et al.*, Phys. Rev. Lett. **97**, 130801 (2006).
[9] A. D. Ludlow *et al.*, Science **319**, 1805 (2008).
[10] M. Takamoto and H. Katori, Phys. Rev. Lett. **91**, 223001 (2003).
[11] Z. W. Barber *et al.*, Phys. Rev. Lett. **96**, 083002 (2006).
[12] F. Sorrentino *et al.*, Phys. Rev. A **79**, 013409 (2009).
[13] P. Wolf *et al.*, Phys. Rev. A **75**, 063608 (2007).
[14] H. Casimir and D. Polder, Phys. Rev. **73**, 360 (1948).
[15] E. M. Lifshitz, Zh. Eksp. Teor. Fiz. **29**, 94 (1956) [Sov. Phys. JETP **2**, 73 (1956)].
[16] J. F. Babb, G. L. Klimchitskaya, and V. M. Mostepanenko, Phys. Rev. A **70**, 042901 (2004).
[17] K. Beloy, V. A. Dzuba, and A. Derevianko, Phys. Rev. A **79**, 042503 (2009).
[18] A. Derevianko, S. G. Porsev, and J. F. Babb, arXiv:0902.3929v1.
[19] V. A. Dzuba and A. Derevianko, arXiv:0908.2278v1.
[20] M. Antezza, L. P. Pitaevskii, and S. Stringari, Phys. Rev. Lett. **95**, 113202 (2005).
[21] J. M. Obrecht *et al.*, Phys. Rev. Lett. **98**, 063201 (2007).
[22] S. G. Porsev and A. Derevianko, Phys. Rev. A **74**, 020502 (R) (2006).
[23] C. I. Sukenik *et al.*, Phys. Rev. Lett. **70**, 560 (1993).
[24] A. Brusch *et al.*, Phys. Rev. Lett. **96**, 103003 (2006).